10-10-2006

Detection of Diffuse Interstellar [O II] Emission from the Milky Way Using Spatial Heterodyne Spectroscopy

E. J. Mierkiewicz
University of Wisconsin-Madison, mierkiee@erau.edu

R. J. Reynolds
University of Wisconsin-Madison

F. L. Roesler
University of Wisconsin-Madison

J. M. Harlander
Saint Cloud State University

K. P. Jaehnig
University of Wisconsin-Madison

The Astrophysical Journal, 650: L63–L66, 2006 October 10

DETECTION OF DIFFUSE INTERSTELLAR [O II] EMISSION FROM THE MILKY WAY USING SPATIAL HETERODYNE SPECTROSCOPY

E. J. Mierkiewicz,[1] R. J. Reynolds,[2] F. L. Roesler,[1] J. M. Harlander,[3] and K. P. Jaehnig[4]

Received 2006 March 15; accepted 2006 August 30; published 2006 September 26

ABSTRACT

Using a newly developed spatial heterodyne spectrometer (SHS), we have obtained the first radial velocity resolved emission-line profiles of diffuse [O II] 3726 and 3729 Å emission lines from the warm (10^4 K) ionized component of our Galaxy's interstellar medium. These [O II] lines are a principal coolant for this widespread, photoionized gas and are a potential tracer of variations in the gas temperature resulting from unidentified heating processes that appear to be acting within the Galaxy's disk and halo. By spectrally isolating for the first time Galactic [O II] from atmospheric [O II] emission, we were able to detect interstellar [O II] out to 20° from the Galactic equator with intensities that range from tens of rayleighs near the Galactic plane to less than 1 rayleigh at high Galactic latitudes. The [O II] line profiles clearly show structure indicating emission along the lines of sight from both local and more distant interstellar gas. Comparisons of the [O II] intensities with the intensities of [N II] 6584 Å and Hα 6563 Å observed with WHAM indicate that the observed variations in [N II]/Hα and [O II]/Hα in the diffuse interstellar gas are consistent with variations in temperature and confirm the value of the [O II] observations as a temperature diagnostic for the WIM.

Subject headings: ISM: general — ISM: structure

1. INTRODUCTION

One of the new results from optical studies of the warm (10^4 K), low-density (10^{-1} cm^{-3}), ionized component of the interstellar medium (i.e., the warm ionized medium [WIM]) is the evidence for variations in the electron temperature within the gas provided by observed spatial variations in the intensity ratios of various nebular forbidden lines (see, e.g., Haffner et al. 1999; Tüllmann et al. 2000; Collins & Rand 2001; Otte et al. 2001; Madsen et al. 2006). These variations could indicate the existence of an additional heating source that is comparable to or greater than the photoionization heating of the gas (see, e.g., Reynolds et al. 1999). Because of the potential consequences for understanding heating and ionization processes within the Galactic halo, it is important to verify that the suggested temperature variations are real and not the result of peculiar ionization effects within the WIM.

There is an emission-line doublet of singly ionized oxygen in the near-ultraviolet spectral region (3727 Å) that is outside the wavelength range accessible to the Wisconsin Hα Mapper (WHAM) but is important for verifying variations in temperature and ionization state within the diffuse ionized gas and for exploring the existence of this additional heating. Our newly developed spatial heterodyne spectrometer (SHS) is capable of detecting [O II] emission from the WIM in the Milky Way, and we report here its first use for measuring interstellar [O II] emission.

[1] Department of Physics, University of Wisconsin–Madison, 1150 University Avenue, Madison, WI 53706; emierk@wisp.physics.wisc.edu, roesler@wisp.physics.wisc.edu.

[2] Department of Astronomy, University of Wisconsin–Madison, 475 North Charter Street, Madison, WI 53706; reynolds@astro.wisc.edu.

[3] Department of Physics, Astronomy and Engineering Science, Saint Cloud State University, 720 Fourth Avenue South, Saint Cloud, MN 56301; harlander@stcloudstate.edu.

[4] Space Astronomy Laboratory, University of Wisconsin–Madison, 1150 University Avenue, Madison, WI 53706; kurt@sal.wisc.edu.

2. TESTING FOR ELECTRON TEMPERATURE VARIATIONS

The temperature and ionization conditions within the WIM appear to differ significantly from conditions within the classical H II regions immediately surrounding O stars. The evidence is provided by observed spatial variations in the intensity ratios of various nebular forbidden lines. For example, the anomalously strong [N II] λ6584/Hα and [S II] λ6716/Hα, and weak [O III] λ5007/Hα emission-line ratios (compared to classical H II regions) indicate a low state of ionization with few ions present that require ionization energies greater than 23 eV (Madsen et al. 2006; Haffner et al. 1999; Rand 1997). While photoionization models incorporating a low-ionization parameter U (the ratio of photon density to gas density) are generally successful in accounting for the low-ionization state of the ions (see, e.g., Domgörgen & Mathis 1994), they fail to explain the observations in detail, in particular the large variations in some of the line ratios. Haffner et al. (1999) have shown that these emission-line observations can be readily explained if the large variations in [N II]/Hα and [S II]/Hα are due primarily to variations in the electron temperature T_e rather than due to variations in the ionization parameter. For the Milky Way, they found that variations in T_e between 7000 and 10,000 K would produce the observed variations in the line ratios.

Therefore, an important question is whether the line ratio variations are indeed due primarily to variations in temperature, and if so, what is the source of this extra heat. Possible radiation transfer effects (Wood & Mathis 2004) and the addition of another ionizing source, such as shocks, turbulent mixing between the hot and warm phases (see, e.g., Slavin et al. 1993), or perhaps X-rays from supernovae (Slavin et al. 2000) can improve the fit to observations (Rand 1997, 1998). However, the behavior of some of the line ratios, particularly the highest observed values of [N II]/Hα and [S II]/Hα, are still not explained by these models. An additional, non-ionizing source of heat such as the dissipation of interstellar turbulence, photoelectric heating by grains, or magnetic reconnection, which will overwhelm the photoionization heating of the gas at the low densities present in the WIM, seems to be required (see,

e.g., Reynolds et al. 1999; Wood & Mathis 2004; Elwert & Dettmar 2005).

The postulated variations in T_e derived from variations in [N II]/Hα can be verified (or refuted) by measuring and comparing the variations in [N II]/Hα with the associated variations in [O II]/Hα. The [O II] transition results from thermal electron excitations to the doublet D state of O^+, 3.3 eV above ground. Since this excitation energy is significantly larger than that of the red [N II] and [S II] lines (1.9 eV), variations in electron temperature will result in a significant and predictable variation in the [O II]/Hα and [N II]/Hα intensity ratios. The O^+ ion is a primary forbidden line coolant (Domgörgen & Mathis 1994) and is the dominant ion of oxygen in the diffuse ionized gas, with O^+/O near unity as implied by both observations of [O I] and [O III] and models (Sembach et al. 2000). This means that [O II] will be relatively bright, comparable to Hα, and that any variations in the intensity ratio [O II]/Hα are the result of variations in the temperature, not the ionization state of oxygen; the hydrogen is nearly fully ionized within this medium (Reynolds et al. 1998). While such analyses have been carried out along lines of sight through the halos of edge-on galaxies (Otte et al. 2001, 2002), the detection of [O II] emission from the Milky Way's WIM was beyond the capability of existing spectrographs.

3. THE [O II] SHS FACILITY

We have designed and built a SHS with the sensitivity and resolving power required to study diffuse [O II] emission from the WIM. In the basic SHS, Fizeau fringes of wavenumber-dependent spatial frequency are produced by a Michelson interferometer modified by replacing the return mirrors with diffraction gratings (Harlander & Roesler 1990; Harlander et al. 1992). These fringes are recorded on a position-sensitive detector and Fourier-transformed to recover a spectrum over a limited spectral range centered at the grating Littrow wavelength. The [O II] SHS combines interferometric and field-widening gains to achieve sensitivities much larger than those of conventional grating instruments of similar size and resolving power, and comparable to the Fabry-Pérot interferometer, but in the near-UV, where WHAM cannot observe.

The [O II] SHS is currently operated at the University of Wisconsin Pine Bluff Observatory, 15 miles west of Madison, Wisconsin. The spectrometer has a resolving power of about 30,000 (10 km s^{-1}) and is coupled to a 24 cm aperture all sky siderostat with a circular field of view on the sky 2° in diameter (Mierkiewicz et al. 2004).

4. OBSERVATIONS

Velocity-resolved observations of the [O II] doublet emission (3726.04, 3728.81 Å) were carried out at sky regions previously mapped by WHAM in [N II] 6584 Å, [S II] 6716 Å, and Hα 6563 Å (Haffner et al. 1999). A series of 10 minute exposures toward target science directions (Table 1) were interspersed with exposures toward calibration regions (e.g., NGC 7000) and toward high Galactic latitude "off" directions of low interstellar [O II] emission. The off directions were used to identify terrestrial emission, which includes [O II] in addition to other airglow lines. The terrestrial λ3729/λ3726 line intensity ratio was measured to be $0.48 \pm 0.05 : 1$, compared to an emission ratio of 1.5 : 1 predicted (and observed) for the interstellar [O II] lines in the low-density limit (Osterbrock 1989). Our formally measured value of $1.54 \pm 0.19 : 1$ for the interstellar [O II] doublet ratio implies that the density of the emitting gas is $\lesssim 10^2$ cm^{-3} (Osterbrock 1989). While not a tight constraint on the WIM density, which has been deduced to be of order 10^{-1} cm^{-3} from comparisons of Hα intensity and pulsar dispersion measures (Reynolds 1991), this is the first direct measurement using a classical density-sensitive optical line doublet.

TABLE 1
OBSERVATIONAL RESULTS

Direction	l (deg)	b (deg)	V_{LSR} (km s^{-1})	$I_{H\alpha}$[a] (R)	[O II]/Hα[b, c]	[N II]/Hα[b]
1	136.2	−06.8	−1.3	2	0.24 ± 0.04	0.33 ± 0.05
2	135.1	−12.7	3.1	3	0.40 ± 0.07	0.52 ± 0.07
3	132.1	−13.6	1.9	4	0.23 ± 0.04	0.38 ± 0.05
4	136.1	−13.6	3.9	2	0.54 ± 0.10	0.63 ± 0.09
5	135.1	−14.4	3.3	2	0.51 ± 0.09	0.59 ± 0.08
6	150.5	−09.3	−2.9	4	0.11 ± 0.02	0.15 ± 0.02
7	150.4	−10.2	0.8	4	0.12 ± 0.02	0.17 ± 0.02
C1[d]	149.0	−0.5	−22	43	0.052 ± 0.009	0.20 ± 0.03
C2[d]	145.2	14.4	2.2	20	0.044 ± 0.008	0.19 ± 0.03

[a] 1 R = $10^6/4\pi$ photons cm^{-2} s^{-1} sr^{-1}.
[b] The uncertainty in the WHAM Hα and [N II] absolute intensity is 10%; there is a 15% uncertainty in the [O II] observations mainly associated with the removal of the atmospheric foreground.
[c] The [O II]/Hα ratio has been normalized to the data at [N II]/Hα = 0.52 via eq. (2), corresponding to a temperature of ~7700 K, pending absolute intensity calibration for our [O II] measurements.
[d] Classical H II region; C1 is ionized by the O9.5 star α Cam, the ionizing source for C2 is tentatively identified as the B1 star LS V +53 12.

The total intensity of the [O II] airglow varied by about a factor of 2 or more over the course of our measurements on any night, with no measurable variation in the doublet ratio. The other airglow features are roughly constant and have nearly constant relative intensities. An average atmospheric foreground template was derived from our off directions with low interstellar [O II] emission. This template was used to remove all of the atmospheric foreground features, except the variable terrestrial [O II] emission, from the science direction spectra.

The interstellar emission profile typically consists of multiple components Doppler-shifted by Galactic differential rotation and random motions between different ionized regions within the WIM. We obtained a least-squares multi-Gaussian fit to our [O II] spectra by requiring the same number of interstellar [O II] Doppler components in each line of the doublet and by requiring the Gaussian velocity components in the [O II] profiles to match the radial velocities and widths of the components in corresponding WHAM [N II] profiles. Five overlapping 1° WHAM [N II] spectra are averaged to simulate the 2° field of view of the [O II] SHS. When fitting the [O II] data, the [N II] widths were scaled to match the resolving power difference between WHAM ($R \sim 25{,}000$) and the SHS ($R \sim 30{,}000$); because of the similar masses of the ions, no correction was needed for the temperature of the gas. The interstellar [O II] λ3729/λ3726 line intensity ratio was set to 1.5 : 1 for each Gaussian velocity component pair. An additional velocity component at rest with respect to the Earth with a corresponding doublet intensity ratio of 0.48 : 1 was included to fit the terrestrial [O II] emission. The paired component areas were varied to obtain a best-fit intensity for each velocity component.

Figure 1*a* is an average of six 10 minute observations from science direction $l = 135.^\circ1$, $b = -12.^\circ7$ after the atmospheric foreground template, which does not include terrestrial [O II] emission, has been subtracted from the spectrum. The solid line in Figure 1*a* is the least-squares Gaussian fit to the resulting [O II] spectrum. In this example, five pairs of velocity components were used in the fit to the doublet: four pairs for the Galactic emission based on the corresponding four-component fit to the WHAM [N II] profile (Fig. 1*c*), and one pair for the terrestrial [O II] emission, indicated in Figure 1*a* by the dotted

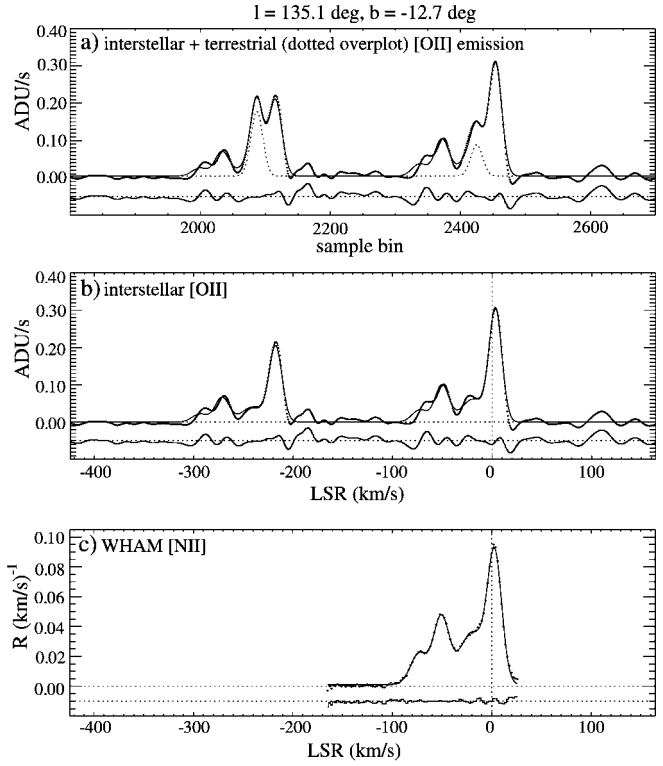

FIG. 1.—Example fit to an [O II] SHS spectrum. (*a*) Fitted [O II] emission (*solid line*). (*b*) Diffuse Galactic [O II] emission free of terrestrial [O II] contributions; emission along the lines of sight from both the local and more distant gas in the Perseus spiral arm (Doppler shifted ~40 km s^{-1} to the blue), is apparent. Note the velocity scale for [O II] is referenced to the 3729 Å line of the doublet. (*c*) WHAM [N II] spectrum. The intensity scale for the WHAM [N II] observation (*c*) is in R (km s^{-1})$^{-1}$; the SHS [O II] intensity (*panels a and b*) is in arbitrary units (but consistent between [O II] spectra).

line overplot. The residuals to the fit (offset from zero for clarity) are also included in Figure 1*a*. Although the terrestrial [O II] emission is unwanted signal, it provides the geocentric rest frame for the spectra. In Figure 1*b*, the terrestrial [O II] emission has been removed, and the coordinate system is transformed to LSR for the 3729 Å line of the doublet. The interstellar [O II] line profiles in Figure 1*b* show structure indicating emission along the line of sight from both the local interstellar gas near the LSR and more distant gas in the Perseus spiral arm and beyond. The total interstellar [O II] doublet emission in Figure 1*b* is ~5*R*.

5. LINE RATIOS

At moderate Galactic latitudes and within the longitude range of our observations ($110° < l < 150°$), the high spectral resolution and sensitivity of the SHS allowed us to resolve kinematically relatively small portions of the Galaxy, without ambiguities associated with the superposition of different areas of the Galaxy along the line of sight. Our observations independently sampled the local diffuse WIM as well as the more distant WIM in the kinematically distinct Perseus spiral arm as a function of distance from the Galactic plane. Only the results for the local emission are discussed below, because the local emission is generally brighter and can be characterized by a single Gaussian component. Also, because path lengths are relatively short and observations are made away from the Galactic plane, extinction is minimal.

The line ratio comparisons of [O II] 3729 Å emission with [N II] and Hα emission confirm that [O II] observations are

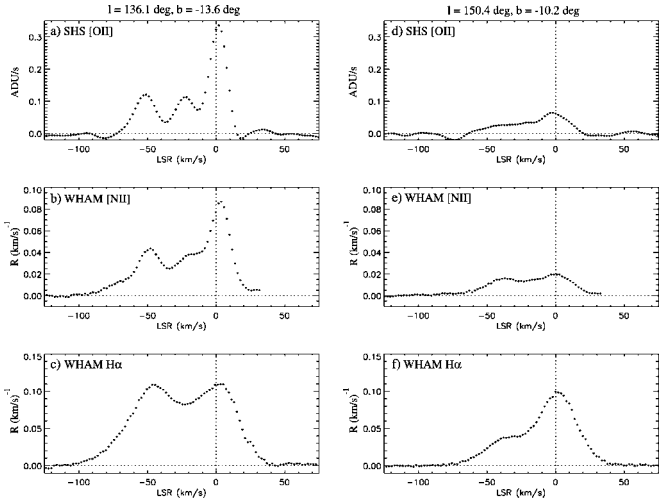

FIG. 2.—SHS [O II] spectra and WHAM [N II] and Hα spectra toward two directions that sample warm ionized gas in both the local and Perseus spiral arms. Toward $l = 136.°1$, $b = -13.°6$ (*left*) the spectra clearly show that the local gas (component near 0 km s^{-1}) has elevated [O II]/Hα and [N II]/Hα, implying a higher temperature, compared to the local component toward $l = 150.°4$, $b = -10.°2$ (*right*). Intensity scales for the WHAM Hα and [N II] observations are in R (km s^{-1})$^{-1}$; the SHS [O II] intensity is in arbitrary units (but consistent between [O II] spectra).

a diagnostic for temperature variations within the diffuse ionized gas. This is illustrated in Figure 2. Figures 2*a* and 2*d* show our spectra of [O II] reduced in the manner discussed in § 4 toward two different directions. These [O II] spectra are then compared to spectra of [N II] (Figs. 2*b* and 2*e*) and Hα (Figs. 2*c* and 2*f*) obtained with WHAM. Note that the widths in the Hα profiles are broader than those of [O II] and [N II] because the width of the emission line from the lighter hydrogen atoms is dominated by thermal broadening. The higher [O II] and [N II] intensities relative to Hα for the low-velocity component (near 0 LSR) toward $l = 136.°1$, $b = -13.°6$ compared to those for the low-velocity component toward $l = 150.°4$, $b = -10.°2$ suggest that the gas toward the former direction has a substantially higher temperature than that toward the latter direction. Not only are [O II]/Hα and [N II]/Hα both higher toward $l = 136.°1$, $b = -13.°6$, but the enhancement in [O II]/Hα is greater than that in [N II]/Hα, just as predicted if the line ratio difference in the two directions were due to a difference in temperature (see eqs. [1] and [2] below).

This conclusion is borne out quantitatively. In Figure 3, our observations of [O II]/Hα are plotted versus [N II]/Hα for the low-velocity (local gas) component toward seven diffuse emission regions between $l = 130°$ and 150° with latitudes between $-6°$ and $-14°$. We have also plotted the data for two bright classical H II regions, LBN 148.11-00.45 (C1) and the α Cam H II region (C2). This plot shows a clear relationship between [O II]/Hα and [N II]/Hα that closely follows the relation predicted by variations in temperature (*solid line*). The solid line in Figure 3 is from the relationships (in photon units):

$$[\text{N II}]/\text{H}\alpha = 9.76 T_4^{0.426} e^{-2.18/T_4} \quad (1)$$

and

$$[\text{O II}]/\text{H}\alpha = 66 T_4^{0.4} e^{-3.87/T_4}, \quad (2)$$

which are derived assuming standard gas phase abundances (Meyer et al. 1997, 1998; Jensen et al. 2005) and ionization

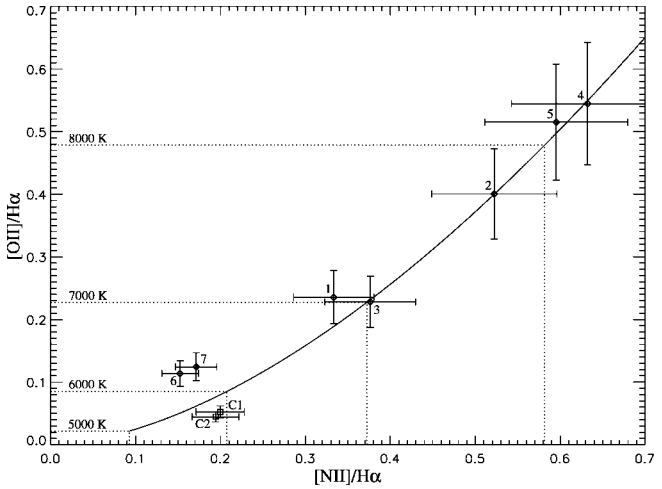

FIG. 3.—[O II]/Hα vs. [N II]/Hα for seven diffuse emission regions (*diamonds*) plus two bright classical H II regions (*squares*). The solid curve is the relationship predicted if the line ratio variations were the result of temperature variations only. The [O II]/Hα ratio has been normalized to the data at [N II]/Hα = 0.52, corresponding to a temperature of ~7700 K, pending absolute intensity calibration for our [O II] measurements. The curve is from eqs. (1) and (2). Refer to Table 1 for the list of data included in this figure.

ratios O^+/O and N^+/N of 1.0 and 0.8, respectively (Otte et al. 2001; Haffner et al. 1999). Because the absolute intensity calibration for our [O II] measurements has not yet been made, the [O II]/Hα ratio has been normalized to the data at [N II]/Hα = 0.52, corresponding to a temperature of ~7700 K. The associated temperatures are also indicated.

The excellent correspondence between the variations in the observed line ratios and the relationship predicted by changes in temperature indicates that for these data the variations in line ratios are consistent with variations in temperature within the ionized gas. Also, the size of these ratio variations is much larger than what could be accounted for by a varying ionization parameter in photoionization models (see, e.g., Hoopes & Walterbos 2003). Note that because the ionization potential of N^+ (29 eV) is significantly less than that of O^+ (35 eV), the somewhat elevated [O II]/Hα (relative to the predicted temperature curve) at low [O II]/Hα and [N II]/Hα (directions 6 and 7 in Fig. 3) could be an indication of ionization effects in which a significant fraction of N is N^{++}. In fact, directions 6 and 7 sample diffuse ionized gas 10°.4 and 10°.2 from the high Galactic latitude O7 star ξ Per, whose hard spectrum could be responsible for a reduction in N^+/N in the nearby gas.

These results confirm the value of [O II] observations as a temperature diagnostic for diffuse ionized gas in the Milky Way. Observations of [N II]/Hα and [S II]/Hα show significant variations in the ratios over large regions of the sky, between ionized super bubbles and the WIM, between the WIM and classical H II regions, and even within the WIM itself (Madsen et al. 2006). Additional [O II] observations will make it possible to explore the extent to which variations in temperature account for these observed spectral differences between different ionized regions.

The authors would like to acknowledge the valuable assistance of L. M. Haffner and G. Madsen. This work is supported by the National Science Foundation through grants AST 01-38228, AST 01-38197, and AST 02-04973.

REFERENCES

Collins, J. A., & Rand, R. J. 2001, ApJ, 551, 57
Domgörgen, H., & Mathis, J. S. 1994, ApJ, 428, 647
Elwert, T., & Dettmar, R. J. 2005, ApJ, 632, 277
Haffner, L. M., Reynolds, R. J., & Tufte, S. L. 1999, ApJ, 523, 223
Harlander, J. M., Reynolds, R. J., & Roesler, F. L. 1992, ApJ, 396, 730
Harlander, J. M., & Roesler, F. L. 1990, Proc. SPIE, 1235, 622
Hoopes, C. G., & Walterbos, R. A. M. 2003, ApJ, 586, 902
Jensen, A. G., Rachford, B. L., & Snow, T. P. 2005, ApJ, 619, 891
Madsen, G., Reynolds, R. J., & Haffner, L. M. 2006, ApJ, in press
Meyer, D. M., Cardelli, J. A., & Sofia, U. J. 1997, ApJ, 490, L103
Meyer, D. M., Jura, M., & Cardelli, J. A. 1998, ApJ, 493, 222
Mierkiewicz, E. J., Roesler, F. L., Harlander, J. M., Reynolds, R. J., & Jaehnig, K. P. 2004, Proc. SPIE, 5492, 751
Osterbrock, D. E. 1989, Astrophysics of Gaseous Nebulae and Active Galactic Nuclei (Mill Valley: University Science Books)
Otte, B., Gallagher, J. S., & Reynolds, R. J. 2002, ApJ, 572, 823
Otte, B., Reynolds, R. J., Gallagher, J. S., & Ferguson, A. M. N. 2001, ApJ, 560, 207
Rand, R. J. 1997, ApJ, 474, 129
———. 1998, ApJ, 501, 137
Reynolds, R. J. 1991, ApJ, 372, L17
Reynolds, R. J., Haffner, L. M., & Tufte, S. L. 1999, ApJ, 525, L21
Reynolds, R. J., Hausen, N. R., Tufte, S. L., & Haffner, L. M. 1998, ApJ, 494, L99
Sembach, K. R., Howk, J. C., Ryans, R. S. I., & Keenan, F. P. 2000, ApJ, 528, 310
Slavin, J. D., McKee, C. F., & Hollenbach, D. J. 2000, ApJ, 541, 218
Slavin, J. D., Shull, J. M., & Begelman, M. C. 1993, ApJ, 407, 83
Tüllmann, R., Dettmar, R. J., Soida, M., Urbanik, M., & Rossa, J. 2000, A&A, 364, L36
Wood, K., & Mathis, J. 2004, MNRAS, 353, 1126